

Magnetic domain wall transitions based on chirality change and vortex position in thin Permalloy™ films

M. Redjail^{a)}

Boston University, ECE Department, 8 Saint Mary's Street, Boston, Massachusetts 02215

A. Kákay

Research Institute for Solid State Physics, H-1525, P.O. Box 49, Budapest, Hungary

M. F. Ruane and F. B. Humphrey

Boston University, ECE Department, 8 Saint Mary's Street, Boston, Massachusetts 02215

The three possible transitions of a wall involving a change of chirality and position of a vortex were previously identified in Permalloy™ using the Kerr effect. These transitions have now been simulated using direct integration of the Landau–Lifshitz–Gilbert equation in a 1 300 000 point Cartesian lattice. One transition is between two C-shaped, same chirality walls whose vortices are on opposite sides. The transition is done via a 32-nm-long pi-VBL structure at the surfaces and at the center via a shape transition 117 nm long. The pi-vertical Bloch line (pi-VBL), which changes chirality along the wall, conducts the flux between the walls of opposite chirality via a vortex structure by letting the magnetization rotate out of the plane of the walls at the center of this vortex. The Néel caps switch chirality via an antivortex flux at one surface and a vortex flux at the other surface. Another transition is a pi-VBL that takes place between two C-shaped, opposite chirality walls whose vortices are on opposite sides of the walls. The transition between the Néel caps of same chirality is a jog at the top surface, while it is a vortex–antivortex pair at the bottom surface.

© 2002 American Institute of Physics. [DOI: 10.1063/1.1454983]

I. INTRODUCTION

The effect of wall transitions (i.e., Bloch lines) on wall motion in thin film magnetic R/W heads was experimentally investigated by Argyle¹ using magneto-optic Kerr effect. These transitions were inferred earlier from a Lorentz microscopy study done by Harrison and Leaver.² Using high resolution Kerr magneto-optic observation of Permalloy films, three plausible wall transitions based on wall chirality change and vortex position were proposed.³ Néel and C-shaped Bloch type sections, which depend on film thickness,^{4,5} were then used to infer the internal structures of these transitions from experimental observations. These transitions will be referred to as T1, T2, and T3, using the naming convention of Ref. 3. Recently, the T2 transition has been simulated in an 80-nm-thick Permalloy film.⁶ It is a pi-vertical Bloch line (pi-VBL) between two “C” shaped wall sections of opposite chirality, vortices on the same side of the wall, and a Néel cap switch at the surfaces. Isolated Bloch wall sections were found to be symmetric at 80 nm thickness;⁵ however, they are C-shaped due to the presence of the long range magnetostatic effect of the transition.

In this work, the detailed (3D) magnetization structure of transitions T1 and T3 are simulated in an 80-nm-thick Permalloy film along with wall transition energies per unit area and transition width. Some details of transition T2 have been included where needed.

II. TECHNIQUE

Simulations were developed as described in Ref. 7 by solving the Landau–Lifshitz–Gilbert (LLG) equation numerically in a regular (xyz) grid with 128 points perpendicular to the wall in (x), 128 points along the wall in (y) and 20 points perpendicular to the plane of the film in (z). The elementary volume is a 4 nm cube, which is less than the 5 nm exchange length for Permalloy. The boundary conditions are such that the wall, in the (yz) plane, is of infinite extent in y . The sample is extended in x , direction normal to the wall, with two semi-infinite magnetic domains saturated along the easy axis y .

The initial magnetization distributions for T1 and T3 were generated by applying an external field to split a 2pi-VBL structure found in Ref. 6. The initial state is then relaxed by solving the LLG at zero external field until the maximum angular spin precession is below 0.004 GHz.

The material parameters are exchange constant $A = 1.0 \times 10^{-6}$ erg/cm, anisotropy field $H_k = 2.5$ Oe, saturation magnetization $4\pi M_s = 10,053$ G, and gyromagnetic ratio $\gamma = -0.0179$ Oe⁻¹ nsec⁻¹. Gilbert damping constant $\alpha = 0.5$ is chosen large to speed up the computations since only equilibrium magnetization states are desired. The film thickness is 80 nm.

III. RESULTS AND DISCUSSION

Figure 1 shows the 3D magnetic wall transitions based on chirality change and vortex position. The volume is 512

^{a)}Electronic mail: makhlof@bu.edu

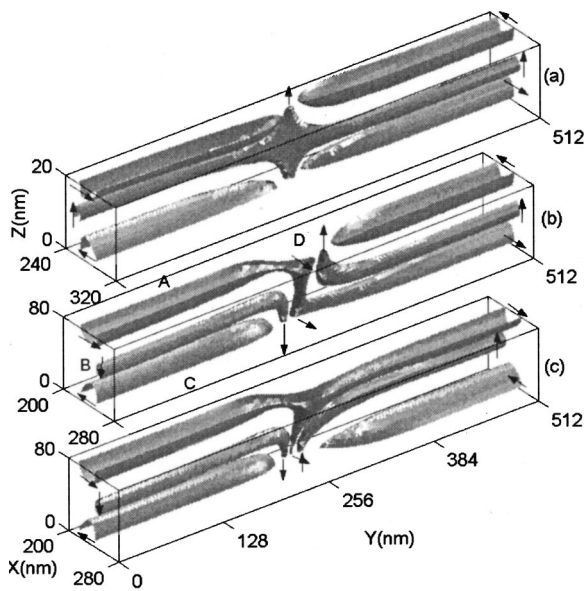


FIG. 1. 3D magnetization configuration in an 80 nm×512 nm×80 nm volume of Permalloy film in a wall with a transition type (a) T1, (b) T2, and (c) T3. Isosurfaces (A) and (C) are Néel caps with $m_x = \pm 0.9M_s$; Isosurface (B) is a Bloch section with $m_z = \pm 0.9M_s$.

nm long in y , 80 nm wide in x , and 80 nm thick in z . Isosurfaces (A) and (C) show the $m_x = \pm 0.9M_s$ component of the magnetization, while (B) shows the $m_z = \pm 0.9M_s$ component. Isosurface (D) for $m_x = +0.9M_s$, a funnel-like volume, represents the core of a pi-VBL. These isosurfaces illustrate magnetization changes as the outer sections of the wall are joined in the wall transition region. The interior volume of each isosurface contains a magnetization whose corresponding component exceeds the $\pm 0.9M_s$ value. Each arrow vector corresponds to the magnetization vector where indicated. Figure 1(a) shows a wall transition of type T1 between two C-shaped, same chirality walls whose vortices are on opposite sides of the walls. A C-shaped section of the wall, at $y=0$ nm, with a $(+z)$ chirality and a vortex on the left is joined, along y , with another C-shaped section, at $y=512$ nm, with a $(+z)$ chirality and a vortex on the right. The transition between the Néel caps of opposite chirality at both surfaces is done via a 32-nm-long pi-VBL structure. The wall transition at the center is a shape transition 117 nm long. The wall energy is increased by 0.38 erg/cm² compared to the energy of a plain wall. Figure 1(b) shows a wall transition of type T2 between two C-shaped, opposite chirality walls whose vortices are on the same side and whose Néel caps are of opposite chirality. This transition was previously simulated⁶ and is included for comparison. A C-shaped section of the wall, at $y=0$ nm, with a $(-z)$ chirality and a vortex on the right is joined, along y , with another C-shaped section, at $y=512$ nm, with a $(+z)$ chirality and a vortex on the right. The wall energy is increased by 0.43 erg/cm², while the pi-VBL width is 88 nm. Figure 1(c) shows a wall transition of type T3 between two C-shaped, opposite chirality walls whose vortices are on opposite sides of the wall. This transition is a pi-VBL. The transition between the Néel caps of same chirality is a jog at the top surface while it is a

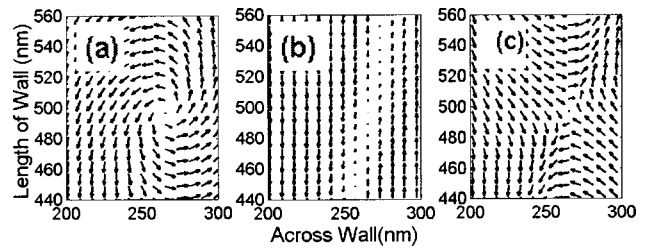


FIG. 2. Magnetization configuration at the top ($z=80$ nm), middle ($z=40$ nm), and bottom ($z=0$ nm) layers in a T1 wall with a pi-VBL.

vortex-antivortex pair at the bottom surface. The transition width is 80 nm. The wall energy is increased by 0.43 erg/cm².

Figure 2 shows the magnetization configuration in an xy plane, parallel to the film plane, containing a T1 transition at the (a) top surface ($z=80$ nm), (b) middle ($z=40$ nm), and (c) bottom surface ($z=0$ nm). On the top surface [Fig. 2(a)] the magnetization rotates in a vortex flux when joining two Néel sections of opposite chirality. At the center of the swirl, the magnetization is out of the plane, normal to the surface. Figure 2(b) shows the middle layer where the two Bloch wall sections of same chirality are joined in the middle with a jog. In Fig. 2(c) the magnetization converges into the same point, an antivortex, as the two Néel sections of opposite chirality are joined at the bottom surface. Identical magnetization configurations were found for the T2 transition at the top and bottom surface,⁶ respectively.

Figure 3 shows the magnetization configuration in an xz cross section normal to the wall plane (yz) at (a) $y=0$ nm, (b) $y=248$ nm, and (c) $y=512$ nm. Néel cap contours for $m_x = \pm 0.9M_s$ (dashed) and Bloch wall contours for $m_z = +0.9M_s$ (solid) show the extent of the Néel and Bloch sections. Figure 3(a) shows a C-shaped domain wall with Néel caps of opposite chirality at the film surfaces, a Bloch wall in the center with a $(+z)$ chirality and an adjoining, right-sided, vortex structure marked by an overshoot of magnetization pointing out of the film plane. The cross section at the center [Fig. 3(b)] shows two symmetric vortices on each side of the wall with a symmetric Bloch wall at the center. Figure 3(c) shows another C-shaped domain wall with Néel caps, but with a Bloch wall of $(+z)$ chirality and a vortex on the left side of the wall. The central Bloch sections are offset by 30 nm in the x direction as the vortices switch sides.

Figure 4 shows the magnetization configuration in an xy cross section parallel to the film plane containing a T3 transition at (a) top surface ($z=80$ nm), (b) middle ($z=40$ nm), and (c) bottom surface ($z=0$ nm).

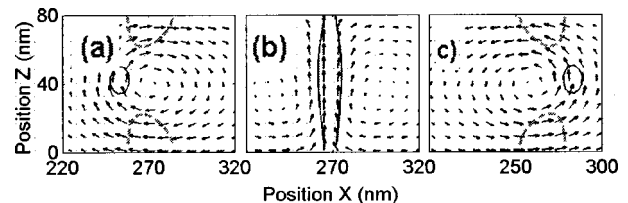


FIG. 3. Projection of magnetization unit vectors on an xz cross section normal to the wall plane (yz) in a T1 transition at (a) $y=0$ nm, (b) $y=248$ nm, and (c) $y=512$ nm; also shown are Néel cap contours for $m_x = \pm 0.9M_s$ (dashed) and Bloch wall contours for $m_z = +0.9M_s$ (solid).

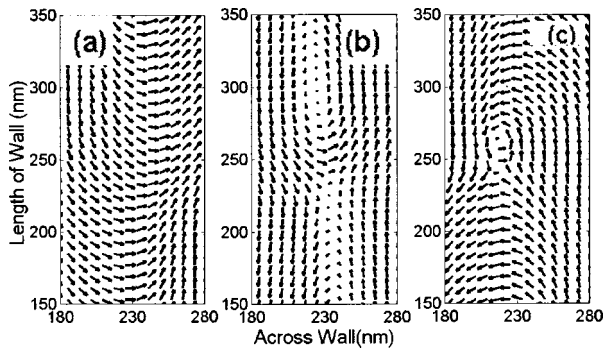


FIG. 4. Magnetization configuration at the top ($z=80$ nm), middle ($z=40$ nm), and bottom ($z=0$ nm) layers in a T3 wall transition with a pi-VBL.

$=40$ nm), and (c) bottom surface ($z=0$ nm). On the top surface [Fig. 4(a)] the transverse magnetization in one Néel section of the wall is joined to another Néel section with a jog in a direction normal to the wall. At the center of the swirl, the magnetization is out of the plane, normal to the surface. Figure 4(b) shows the middle plane where the magnetization rotates out of the plane (yz) of the wall when two Bloch wall sections of opposite chirality are joined. An identical magnetization configuration was found for the T2 transition at the same middle plane.⁶ In Fig. 4(c) the transition between the Néel caps is a vortex-antivortex pair at the bottom surface.

Figure 5 shows the magnetization configuration in an xz cross section normal to the wall plane (yz) in a T3 transition at (a) $y=0$ nm, (b) $y=248$ nm, and (c) $y=512$ nm. Néel cap contours for $m_x = \pm 0.9M_s$ (dashed) and Bloch wall contours for $m_z = \pm 0.9M_s$ (solid) show the extent of the Néel and Bloch sections. Figure 5(a) shows a C-shaped domain wall with Néel caps of opposite chirality, a Bloch wall with a $(-z)$ chirality and an adjoining, left-sided, vortex structure marked by an overshoot of magnetization pointing out of the film plane. The cross section at the center of the T3 transition [Fig. 5(b)] shows the core of the pi-vertical Bloch line, wide at the top and narrow at the bottom, whose extent is delimited by the $m_x = +0.9M_s$ contour. Figure 5(c) shows another C-shaped domain wall with Néel caps, but with a Bloch wall of $(+z)$ chirality and a vortex on the right side of the wall. The central Bloch sections are offset by 30 nm in the x direction.

Figure 6 shows the polar angle θ , measured counterclockwise from the $(-z)$ axis, along a line at the top, center,

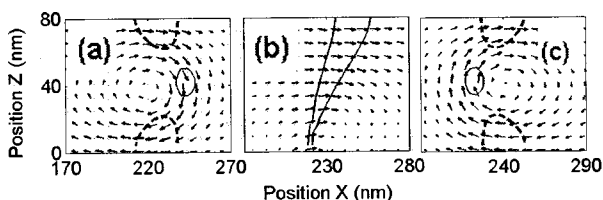


FIG. 5. Projection of magnetization unit vectors on an xz cross section normal to the wall plane (yz) in a T3 transition at (a) $y=0$ nm, (b) $y=248$ nm, and (c) $y=512$ nm; also shown are Néel cap contours for $m_x = \pm 0.9M_s$ (dashed) at surfaces and Bloch wall contours for $m_z = \pm 0.9M_s$ (solid).

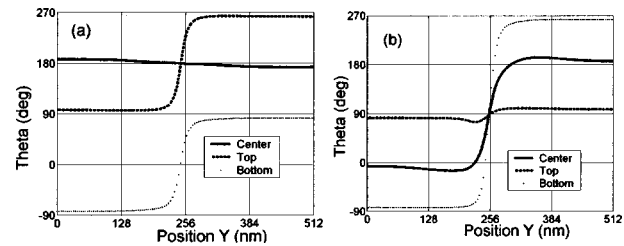


FIG. 6. Magnetization polar angle θ at the top, center and bottom layers of the wall center slice as a function of position along the domain wall; (a) a T1 transition and (b) a T3 transition.

and bottom layers of the wall center. For the T1 transition [Fig. 6(a)] the spins at the center rotate away by $\pm 7^\circ$ from the $(+z)$ chirality but remain, on average, saturated in the $(+z)$ direction. At the surfaces, the spins rotate 180° starting in a Néel cap with $(+x)$ chirality at the top surface ($-x$ chirality at the bottom) and end in another Néel cap with $(-x)$ chirality ($+x$ chirality at the bottom). In the T1 transition region, the spins rotate counterclockwise, “up” out of the plane of the film at the top surface, and “down” out of the plane of the film at the bottom surface.

The T3 transition (a pi-VBL), [Fig. 6(b)] starts and ends in Bloch sections with opposite chirality through a 180° rotation (solid line) of its center spin, passing through a shortened Néel section with a $(+x)$ chirality, the center of the pi-VBL. At the top surface, the spins remain saturated in average within $\pm 7^\circ$ excursion away from the $(+x)$ chirality except at the transition region, where an excursion of -15° out of the plane and “down” was computed (dashed line). At the bottom surface, the spins rotate counterclockwise 360° (dotted line) starting at a $(-x)$ Néel cap at $y=0$ nm, out of the plane joining the $(-z)$ Bloch section, back in plane in a $(+x)$ Néel cap at $y=256$ nm, continuing up, joining the $(+z)$ Bloch section to end in the $(-x)$ Néel cap at $y=512$ nm.

The width of the pi-VBL at the surface for T1 transition and at the center for the T3 transition is determined by extrapolation of the linear portion of the curve to 0° and 180° in the surface layer. The widths are 256 nm for a T1 transition at the center but only 28 nm for corresponding pi-VBLs at the surfaces. The width is 45 nm for the T3 pi-VBL transition.

ACKNOWLEDGMENTS

The authors wish to thank Seagate Technologies, Minneapolis, Minnesota for partial support.

- ¹B. E. Argyle, B. Petek, M. E. Re, F. Suits, and D. A. Herman, *J. Appl. Phys.* **63**, 4033 (1988).
- ²C. G. Harrison and K. D. Leaver, *Phys. Status Solidi A* **15**, 415 (1973).
- ³R. Schafer, W. K. Ho, J. Yamasaki, A. Hubert, and F. B. Humphrey, *IEEE Trans. Magn.* **27**(4), pp. 3678 (1991).
- ⁴M. Redjidal, T. Trunk, M. F. Ruane, and F. B. Humphrey, *IEEE Trans. Magn.* **36**, 3071 (2000).
- ⁵T. Trunk, M. Redjidal, A. Kakay, M. F. Ruane, and F. B. Humphrey, *J. Appl. Phys.* **89**, 7606 (2001).
- ⁶M. Redjidal, A. Kakay, T. Trunk, M. F. Ruane, and F. B. Humphrey, *J. Appl. Phys.* **89**, 7609 (2001).
- ⁷M. Redjidal, P. W. Gross, A. Kazmi, and F. B. Humphrey, *J. Appl. Phys.* **85**, 6193 (1999).